Behavioral/Systems/Cognitive

A Mammalian Retinal Bipolar Cell Uses Both Graded Changes in Membrane Voltage and All-or-Nothing Na^+ Spikes to Encode Light

Shannon Saszik and Steven H. DeVries
Departments of Ophthalmology & Physiology, Northwestern University Feinberg School of Medicine, Chicago, Illinois 60611

Barlow (1953) studied summation in ganglion cell receptive fields and observed a fine discrimination of spatial information from which he inferred that retinal interneurons use analog signals to process images. Subsequent intracellular recordings confirmed that the interneurons of the outer retina, including photoreceptors, horizontal cells, and bipolar cells, respond to light with slow, graded changes in membrane potential. Analog processing may enable interneurons to discriminate fine gradations in light intensity and spatiotemporal pattern, but at the expense of the speed, temporal precision, and threshold discrimination that are characteristic of all-or-nothing Na^+ spikes. We show that one type of mammalian On bipolar cell, the ground squirrel cb5b, has a large tetrodotoxin (TTX)-sensitive Na^+ current. When recorded from in the perforated patch configuration, cb5b cells can signal the onset of a light step with 1–3 all-or-nothing action potentials that attain a peak amplitude of −10 to −20 mV (peak width at half-height equals 2–3 ms). When exposed to a continuous, temporally fluctuating stimulus, cb5b cells generate both graded and spiking responses. Cb5b cells spike with millisecond precision, selecting for stimulus sequences in which transitions to light are preceded by a period of darkness. The axon terminals of cb5b bipolar cells costratify with the dendrites of amacrine and ganglion cells that encode light onset with a short latency burst of spikes. The results support the idea that a spiking On bipolar cell is part of a dedicated retinal pathway for rapidly and reliably signaling dark to light transitions.

Introduction

The neurons of the outer retina process light stimuli with graded changes in membrane potential (Barlow, 1953; Werblin and Dowling, 1969; Baylor and Fuortes, 1970; Kaneko, 1970). Photoreceptors signal the absorption of light with a membrane hyperpolarization that decreases the rate of glutamate release at the synaptic terminal (Dowling and Ripps, 1973). This decrease leads to a graded hyperpolarization in horizontal and Off bipolar cells and a depolarization in On bipolar cells (Werblin and Dowling, 1969).

Graded signals can transmit more information than spike trains (de Ruyter van Steveninck and Laughlin, 1996; Juusola and French, 1997), and thus their prevalence in the outer retina can be beneficial, especially since electrotonic degradation is minimal over the short distances involved. However, even under these conditions, signaling with all-or-nothing action potentials may sometimes be advantageous. For example, action potentials can propagate rapidly through neuronal networks, both across cell processes and at synapses, whereas graded voltage changes propagate relatively slowly through the retina (Baylor and Fettiplace, 1977). In the retina, rapid propagation may be useful for signaling a change in the visual scene. In addition, unlike graded responses, spikes typically occur when a strong stimulus produces a depolarization that exceeds threshold. A spike threshold may allow retinal interneurons to encode rare, but important stimuli.

While the outer retinal neurons are considered to be nonspiking, many contain voltage-dependent Na^+ currents that can shape light responses. For example, isolated horizontal cells have a large Na^+ current (1–2 nA) (Shingai and Christensen, 1983), but are not thought to spike in the retina due to shunting by glutamate-gated and K^+ conductances (Lasater, 1986; Shingai and Christensen, 1986). Instead, the Na^+ current increases the rate of membrane depolarization at light-off (Lasater, 1986). Some bipolar cells in the goldfish (Zenisek et al., 2001), salamander (Ichinose et al., 2005), and rat (Pan and Hu, 2000) have relatively small (<100 pA) currents that can either potentiate light responses or, under certain conditions, generate 5–10 mV spikes (Ichinose and Lukasiewicz, 2007). Larger Na^+ currents (200–400 pA) were found in 5–10% of dissociated rat bipolar cells (Pan and Hu, 2000), and in one or more bipolar cell subtypes in rat retinal slices (Ma et al., 2005). The presence of a large Na^+ current in the mammal suggests that some bipolar cells could signal light with all-or-nothing Na^+ action potentials, but light-triggered Na^+ spikes have not been observed.

We now show that a type of ground squirrel bipolar cell, the cb5b, has a large, transient Na^+ current and can fire a 40 mV action potential with a short latency at light-onset or during a

Received June 16, 2008; revised Nov. 3, 2011; accepted Nov. 5, 2011.

Author contributions: S.H.D. designed research; S.S. and S.H.D. performed research; S.S. and S.H.D. analyzed data; S.H.D. wrote the paper.

We are indebted to Dr. Charles Ratliff for generating the m-sequence and to the National Institutes of Heath (S.H.D., Grant EY18204; S.S., Grant EY15967) and Research to Prevent Blindness for support.

Correspondence should be addressed to Dr. Steven H. DeVries, Department of Ophthalmology, Tarry 5-715, Northwestern University Medical School, 303 E. Chicago Avenue, Chicago, IL 60611. E-mail: s-devries@northwestern.edu.

DOI:10.1523/JNEUROSCI.2739-08.2012

 0270-6474/12/320297-11$15.00/0

continuously fluctuating stimulus after dark to light transitions. cb5b cell axon terminals costratify with the dendrites of ganglion cells that fire a burst of spikes at light-onset. We speculate that a bipolar cell that uses Na^+ spikes to encode extreme changes in the visual scene may trade the steady information carrying capacity inherent in graded signaling for the ability to elicit a rapid and reliable response in transient-type ganglion cells.

Materials and Methods

Preparation and electrophysiology. All procedures were approved by the Northwestern University Animal Care and Use Committee. The procedures for making ground squirrel (of either sex, *Ictidomys tridecemlineatus*, formerly *Spermophilus tridecemlineatus*; Helgen et al., 2009) retinal slices (DeVries, 2000) and flat-mounts (Szmajda and DeVries, 2011) have been described. For recording, the extracellular solution contained the following (in mM): 115 NaCl, 25 $NaHCO_3$, 3.1 KCl, 2.0 $CaCl_2$, 2.5 $MgSO_4$, 6 glucose, 1 Na-pyruvate, 1 Na-lactate, 1 Na-malate, 1 Na-succinate, 0.05% phenol red, and was equilibrated with 5% CO_2/95% O_2 to a pH of 7.4. Tissue was mounted on a Zeiss Axioskop 2 microscope equipped with a 63×/numerical aperture water-immersion objective and continuously superfused at a rate of 0.2 ml-min^{-1} at 31−32°C. The standard patch pipette solution contained the following (in mM): 120 KCl, 0.5 EGTA, 2 $MgSO_4$, 10 HEPES, 10 NaCl, 5 ATP, 0.5 GTP, and 5 $MgCl_2$. The pH was adjusted to 7.4 with KOH. During measurements of bipolar cell Na^+ currents, K^+ currents were suppressed by substituting 100 mM CsCl and 20 mM tetraethylammonium chloride for internal KCl, and Ca^{2+} currents were suppressed by adding 1 μM isradipine (Tocris Bioscience) to the external solution. Measurements of bipolar cell light responses were obtained with perforated patch recording. Stock solutions of amphotericin B (100 mg-ml^{-1} in dimethyl sulfoxide) or gramicidin D (10 mg-ml^{-1} in methanol; Akaike, 1996) were prepared daily. Final concentrations of amphotericin (0.3–1.0 mg-ml^{-1}) or gramicidin (0.1–0.4 mg-ml^{-1}) were obtained by dilution into the KCl-based pipette solution followed by brief sonication (30 s). Both perforating agents produced similar experimental results, but amphotericin was preferred due to a more rapid and reliable effect. For recording from ganglion cells, 0.5 mM QX 314 (*N*-(2,6-Dimethylphenylcarbamoylmethyl)triethylammonium) bromide (Tocris Bioscience) was included in the intracellular solution. In addition, potassium methyl sulfate was substituted for KCl ($E_{Cl} \approx -70$ mV). Recordings obtained with intracellular solutions that contained a high Cl^- concentration were not corrected for an estimated liquid junction potential of <2 mV. Recordings with other intracellular solutions were corrected using the program jp (www.physio.unr.edu/faculty/kenyon/index.asp). Sulforhodamine 101 (0.5 mM; Invitrogen) was added to visualize bipolar cells under epifluorescence. Lucifer yellow (1%) or Neurobiotin (1–2%; Vector Laboratories) was also added if the tissue was to be fixed and used in confocal microscopy. TTX (2 μM; Tocris Bioscience) was applied by puffer. Chemicals were from Sigma-Aldrich unless otherwise specified. Holding potentials were −70 mV unless specified. All values are mean ± SD. Statistical significance was determined with a two-tailed Wilcoxon rank test which is used to assess whether the means of two independent samples differ.

Recordings were obtained with an Axopatch 200B amplifier (Molecular Devices). Amplifier output was filtered at 5 kHz with a 4-pole Bessel filter and digitized at 10–17 kHz with an ITC-18 interface (HEKA Instruments) controlled by a G4 PowerMac computer running custom software (IgorPro 5.0; WaveMetrics). For all bipolar cell recordings, the pipette capacitance artifact was minimized by coating the tip with Parafilm (American National Can) and adjusting pipette capacitance compensation. For characterizing Na^+ current activation and inactivation kinetics during whole-cell recordings, pipette series resistance (R_p) and cell membrane capacitance (C_m) were neutralized and prediction and correction were set at 60–70%. For determining the $V_{1/2}$ of Na^+ channel activation and inactivation, normalized conductance plots were obtained for individual cells, and the results were then pooled and fitted with a Boltzmann function. Na^+ currents were isolated by TTX subtraction when explicitly stated. In all other instances, the amplitude of the Na^+ current was estimated during a voltage-clamp step from −70 to −30 mV by measuring the difference between the current peak and the subsequent steady current level. Peak currents were ~10% larger when estimated by control responses alone when compared with those obtained by TTX-subtraction. The small difference was ignored. Perforated patch recordings were performed in the I-clamp fast mode. R_p compensation was not used insofar as a steady decrease in pipette series resistance from ~800 to 70 MΩ during the first 30 min of recording would have necessitated repeated adjustments and might have created artifacts due to periodic overcompensation. R_p was calculated by measuring the peak of the capacitance transient in voltage clamp at the end of a 20 mV step from −70 mV. As a check, the calculated R_p and the time constant of the subsequent current decay were used to determine C_m. C_m determined in this way was close (2–10 pF) to that obtained from bipolar cells using responses to step current injection in the whole-cell recording configuration (6–10 pF; DeVries et al., 2006). We did not use steady current injection to change resting potential. When recording light responses, dissection was done under dim red light and slices were viewed under infrared illumination with a microscope-mounted CCD camera (Watec). Bipolar cells were stimulated by flashes and steps of light that were produced either by the microscope mercury arc lamp (Zeiss HBO 100) or an LED stimulator. Light from the mercury lamp was passed through a series of neutral density filters (Melles Griot), a computer-controlled shutter (Uniblitz, Vincent Associates), and a bandpass filter (496 ± 10 nm; #51006x, Chroma Technology). During some experiments on bipolar cells and all experiments on ganglion cells, light steps were generated by an LED (λ_{max} = 574 nm) mounted on a microscope video port. LED intensity was controlled with pulse-width modulation and could be varied over a 100-fold range (Light, 2009). When necessary, greater attenuation was provided by placing neutral density filters in the light path. Light intensities were calibrated with a photodiode detector (International Light) placed at the location of the recording chamber and converted into units of photons-μm^{-2}-s^{-1} at the λ_{max} of the green cone pigment (517 nm; Kraft, 1988) using a Dartnall nomogram (Dawis, 1981). The light intensities for individual experiments are specified in the text and figure legends.

An m-sequence (Reid et al., 1997; Schroeder, 2009) was used to generate a binary light stimulus that had a minimum interval of either 7.5 or 15 ms and a duration of either 7.67 or 15.34 s. For these experiments, data were filtered at 2 kHz and digitized at either 10 or 5 kHz. Linear filters for graded responses were obtained by cross-correlating the stimulus waveform with the bipolar cell voltage response. Linear filters for spiking responses were obtained by cross-correlating the stimulus waveform with a binarized version of the bipolar cell voltage response. Spiking bipolar cell responses were binarized by setting all voltages above a fixed threshold to 1 and below the threshold to 0. Thresholds were set by eye at a level that intersected only narrow transient and not broader graded responses. A biphasic index for the filter was calculated by taking the absolute value of the negative peak amplitude, the positive peak amplitude being normalized to 1.

Immunocytochemistry. Cells were labeled with Neurobiotin tracer (Vector Laboratories) during recording. Retinas were fixed overnight with 4% paraformaldehyde at 4°C. Immunocytochemical methods have been described (Li and DeVries, 2006). Retinas were labeled with antibodies raised against calbindin (slice, 1:500; whole mount, 1:250) and protein kinase C α (PKC; slice, 1:1000; whole mount, 1:500; Santa Cruz Biotechnology). Primary antibodies were visualized with Cy5-donkey anti-mouse (1:100, Jackson ImmunoResearch), Cy3-donkey anti-rabbit (1:100, Jackson ImmunoResearch), and Alexa Fluor 488-conjugated streptavidin (1:100, Invitrogen). Images were acquired with a Zeiss LSM-510 META confocal microscope.

For comparing the intensity of calbindin and PKC labeling in cb5 bipolar cells among different slices, the confocal microscope laser power and photomultiplier gain and threshold were adjusted so that the output filled the entire range of the digitizer. Different settings were used for each slice. For each image, somatic labeling was isolated by applying a mask, and the average soma intensity was then measured in each channel. Raw average intensities were normalized by first calculating the intensity ratio of PKC to calbindin labeling in the recorded cell and then in nearby unrecorded cb5a and cb5b cells. Next, the cb5a and cb5b ratio values

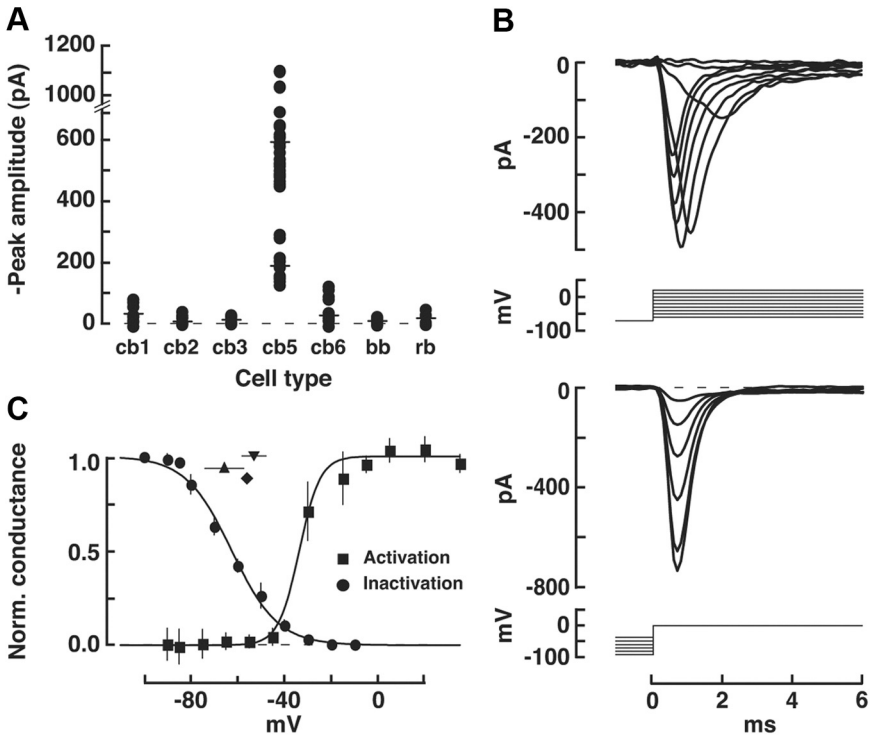

Figure 1. cb5 bipolar cells have a large, transient Na^+ current. ***A***, Peak amplitude of the TTX-sensitive current in a series of bipolar cells (circles; $n = 101$) recorded in retinal slices. Cells were held at −70 mV and stepped to −30 mV. Horizontal lines indicate mean peak current. Cells were identified from fluorescence images obtained immediately after whole-cell recording. Cell types are ordered according to axon ramification depth in the IPL. ***B***, Top, The membrane voltage of a cb5 bipolar cell was held at −70 mV and stepped to a series of potentials between −60 and 20 mV in 10 mV increments. The TTX-sensitive current is shown. The voltage command is plotted below. Bottom, Membrane voltage was maintained in 10 mV increments between −90 and −10 mV and stepped to a test potential of 0 mV. The TTX-sensitive current during steps from −90 to −40 mV is shown. Upper and lower sets of traces are from separate cells. ***C***, Plots of channel activation and inactivation versus membrane voltage for cb5 cells during a step from −70 to −30 mV. Points show mean conductance values obtained by pooling measurements from 10 cells in the group with larger peak Na^+ currents. The fits were obtained from a Boltzmann equation. For comparison, individual symbols plot the mean resting potentials of cb5 cells with large Na^+ currents measured during subsequent experiments under three recording conditions: whole-cell recording (upward triangle), amphotericin perforated patch recording (diamond), and gramicidin perforated patch recording (downward triangle). Both vertical and horizontal bars show SD. Bars overlap with the symbol when not visible.

were converted to 0 and 1, respectively, first by subtraction and then by division. The conversion factors were applied to the intensity ratio in the recorded cell.

Plots of label intensity versus inner plexiform layer (IPL) depth were calculated from a *z*-stack that spanned the IPL at 1 μm intervals. A 10 × 10 μm square was selected for analysis and the average values for each of the three labels was calculated in each optical section. The percentage overlap between ganglion or amacrine cell dendrites and the terminals of cb5b or cb5a cells was calculated as 100 × (peak area[PKC labeling ∩ calbindin labeling ∩ Neurobiotin labeling]/peak area[Neurobiotin labeling]).

Results

TTX-sensitive currents in bipolar cells

Ground squirrel bipolar cells can be subdivided into 10 or more anatomical types based on the level of their axon termination in the IPL (West, 1976; Linberg et al., 1996; DeVries, 2000; Cuenca et al., 2002; Li and DeVries, 2006; Puller et al., 2011). We compared the TTX-sensitive membrane currents in three Off bipolar cell types (cb1, cb2, cb3) and 4 On bipolar cell types (cb5, cb6, bb, rb) by stepping membrane voltage from −70 to −30 mV. Cells were labeled with a fluorescent tracer during recording and identified by their morphology afterward. The mean amplitude of the TTX-sensitive current in most types of bipolar cells was smaller than −25 pA (Fig. 1*A*); indeed, currents in four bipolar cell types (cb2, cb3, bb, rb) were not significantly different from 0 pA ($p < 0.01$). However, one subtype, the cb5, had currents that could exceed −1000 pA. Cells with cb5-like morphology could be divided into at least two groups, one with larger (−592 ± 163 pA, $n = 26$) and one with smaller (−193 ± 53 pA, $n = 19$) peak currents.

We characterized the voltage dependence and kinetics of the TTX-sensitive current in the upper group of cb5 cells. The voltage dependence of channel activation was obtained by maintaining membrane voltage at −70 mV and then stepping to a series of more depolarized potentials. At its maximum, the inward current in the cell in Figure 1*B* (top) peaked at ~−500 pA and then rapidly decayed (with an exponential time constant, τ, equal to 2.2 ± 0.6 ms, $n = 10$) to a much smaller steady level (<5% of the peak). A plot of conductance versus step voltage for the sample ($n = 10$; Fig. 1*C*) showed that activation was half-maximal ($V_{1/2}$) at −34.6 mV and the effective gating charge, *z*, was 5.9. The voltage dependence of channel inactivation was obtained during steps to a test potential of 0 mV from a series of maintained potentials between −90 and −20 mV (Fig. 1*B*, bottom). The $V_{1/2}$ for inactivation (Fig. 1*C*) was −62.4 mV ($z = 4.6$). The sensitivity to TTX, rapid kinetics, and activation and inactivation curves are characteristic of transient Na^+ currents (Hille, 2001).

cb5 bipolar cells can be divided into two costratifying types based on their immunolabeling patterns and dendritic field tiling (Cuenca et al., 2002; A. Light, Y. Zhu, J. Shi, S. Saszik, S. Lindstrom, L. Davidson, V. Chiodo, W. Hauswirth, W. Li, and S. DeVries, unpublished observation). One type, the cb5b, labels with antibodies against calbindin (calb) and PKCα (PKC), whereas the other type, the cb5a, is calb positive and PKC negative. We wanted to determine whether there was a correspondence between the higher and lower Na^+ current amplitude groups and the cb5a and cb5b cells. To do this, we measured the peak Na^+ current amplitude in 11 cb5 cells during a test step from −70 to −30 mV (Fig. 2*A*,*F*). Slices were then fixed and immunolabeled for Neurobiotin tracer (included in the pipette solution), PKC, and calb. Examples of recorded and labeled bipolar cells with cb5 morphology are shown in Figure 2. A bipolar cell with a −585 pA Na^+ current (Fig. 2*A*) was triply labeled for tracer, calb, and PKC (Fig. 2*B–E*). A similar labeling pattern was obtained for the bipolar cells in Figure 1*B*. A bipolar cell with a smaller Na^+ current (−225 pA; Fig. 2*F*) was calb positive and PKC (Fig. 2*G–J*) negative.

We quantified the intensity of calb and PKC labeling in the recorded cb5 bipolar cells and, for comparison, in nearby unrecorded cb5a and cb5b cells. With a few exceptions, unrecorded cb5 cells could be divided into two groups (Fig. 3*A*): One group labeled strongly for both calb and PKC and thus were cb5b type;

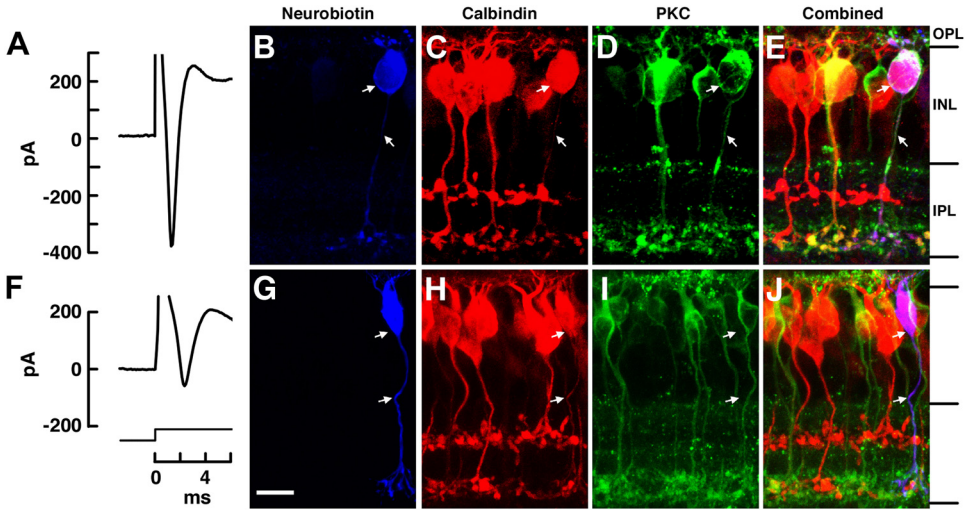

Figure 2. Peak Na^+ current amplitude and immunolabeling for calb and PKC in cb5 cells. The recording pipette contained Neurobiotin. ***A***, A transient inward current in a bipolar cell during a step from −70 to −30 mV. ***B–D***, Images of the retinal slice showing labeling for Neurobiotin, calb, and PKC. ***E***, The superimposed images from *B–D*. The recorded cell is positive for calb and PKC. ***F***, A smaller transient inward current in a different bipolar cell. ***G–J***, The recorded cell is $calb^+/PKC^-$. Scale bar, 5 μm. Arrows mark the locations of tracer-labeled somas and axons. Outer plexiform layer (OPL); Inner nuclear layer (INL).

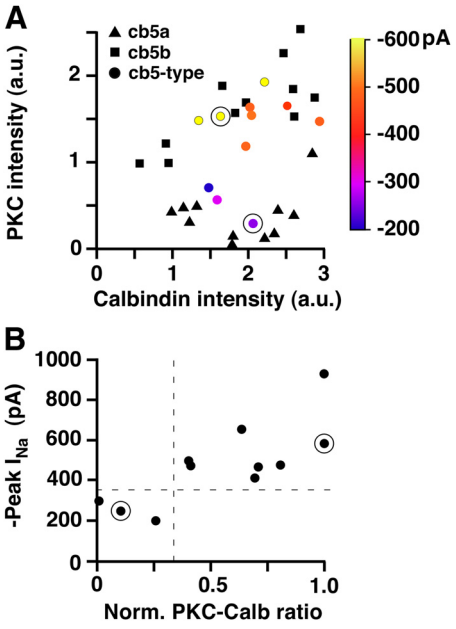

Figure 3. Calb and PKC labeling is associated with a cell having a large Na^+ current. ***A***, The intensity of PKC labeling is plotted against the intensity of calb labeling for the somas of recorded (filled circles) and neighboring, unrecorded (black symbols) cells. Unrecorded cells with nearly equal PKC and calb label intensities were classified as cb5b (squares), whereas those with a high ratio of calb to PKC label intensity were classified as cb5a (triangles). Na^+ current amplitude for the recorded cells is indicated by circle color (scale at right). ***B***, Plot of Na^+ current amplitude verses PKC to calb intensity ratio, normalized by comparison with nearby cb5a and cb5b cells. The excessive number of recorded cb5b cells in the sample is likely due to bias insofar as the ratio of cb5b:cb5a cells in the intact retina is only 1.4 (A. Light, Y. Zhu, J. Shi, S. Saszik, S. Lindstrom, L. Davidson, V. Chiodo, W. Hauswirth, W. and Li, S. DeVries, unpublished observations). The points corresponding to the results from the cells shown in Figure 2 are circled. Intensity is expressed in arbitrary units (a.u.).

whereas, a second group labeled strongly for calb and weakly for PKC and were cb5a type. Three cells may comprise a third group that labeled equally but moderately for both calb and PKC. These cells were judged to be cb5b type. Eight of the recorded cells had cb5b-like labeling ($calb^+/PKC^+$) and Na^+ currents larger than −400 pA, whereas the remaining three had cb5a-like labeling ($calb^+/PKC^-$) and Na^+ currents smaller than −400 pA (Fig. 3*A*). The relative intensities of calb and PKC labeling were optimized for viewing in individual slices and, in this sample, varied across slices. We addressed this source of variability by calculating the ratio of PKC to calb labeling intensity for the recorded cell and nearby cells in the same slice that were judged to be cb5a- or cb5b-type. We used the ratios in neighboring cells to normalize the ratio in the recorded cell, and plotted this value on the abscissa versus Na^+ current on the ordinate (Fig. 3*B*). The cells with smaller Na^+ currents had cb5a-like labeling, whereas those with larger currents had cb5b-like labeling. Henceforth, cells with Na^+ currents larger than −400 pA or that are $Calb^+/PKC+$ will be called cb5b cells; $calb^+/PKC^-$ cells or cells with Na^+ currents smaller than −400 pA will be called cb5a cells.

Current injections produce action potentials in cb5b bipolar cells

Having a large Na^+ current does not guarantee that a neuron can produce action potentials. For example, a relatively depolarized resting membrane potential could inactivate a substantial fraction of the Na^+ channels. We recorded the resting potential of cb5b bipolar cells in the dark-adapted retina. On average, these cells rested at −66.5 ± 8.5 mV (n = 8), a potential at which approximately half of the Na+ channels present are available for activation (Fig. 1*C*). We next determined whether cb5b bipolar cells could generate all-or-nothing action potentials during current injections (Fig. 4). The bipolar cell in Figure 4*A* had a transient inward current of −735 pA at the onset of a voltage step from −70 to −30 mV. In current clamp, the cell rested at a membrane potential of −70 mV. Step current injections of 20–30 pA produced graded membrane depolarizations, whereas current injections of 40 pA or more led to a 35–40 mV rapidly rising and decaying voltage transient (width at half-height = 1.4 ms). A total of 10 cells in the sample had transient inward currents exceeding −400 pA during a voltage step and were thus classified as cb5b type. In current clamp, all 10 cells demonstrated a nonlinear membrane depolarization during current steps of 30–75 pA, indicative of spike generation (results from six representative cells are plotted in Fig. 4*D*, top; the current step that exceed the spike

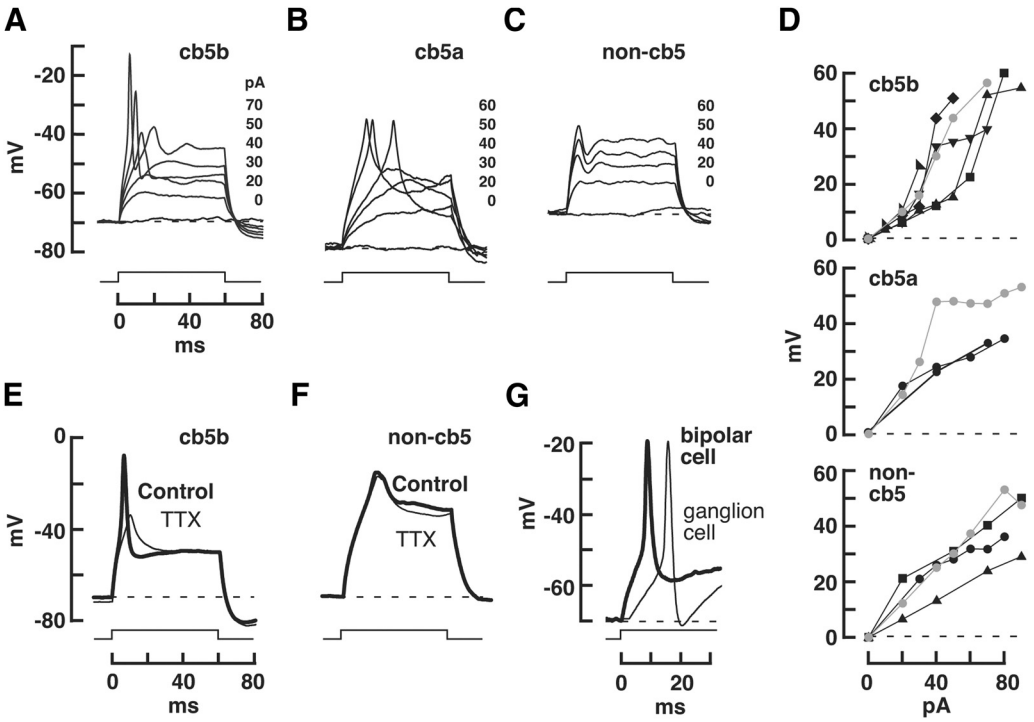

Figure 4. Current injections elicited action potentials in cb5 bipolar cells. ***A***, Membrane voltage response of a cb5b bipolar cell during step current injections of 0–70 pA (listed at right, corresponding to responses of increasing amplitude). The timing of the current pulse is shown below. ***B***, Membrane voltage response of a cb5a bipolar cell (peak transient response equaled −120 pA during a voltage-clamp step from −70 to −30 mV) to a series of current injections. ***C***, Response of an On sublamina stratifying bipolar cell with a negligible Na^+ current to a series of current injections. ***D***, Plot of peak responses versus injected current for cb5b (top), cb5a (middle), and representative non-cb5 On bipolar (bottom) cells. Gray circles plot the responses of the cells in ***A–C***. ***E***, Response of a cb5b cell to a step current injection (90 pA) before and during TTX exposure. ***F***, Response of a non-cb5 cell to a 70 pA current injection before and during TTX exposure. ***G***, Superimposed cb5b bipolar and ganglion cell action potentials obtained during step current injections in a slice. Ganglion cell trace displaced upward by 2 mV from its resting potential. Cells were grouped into categories, cb5a, cb5b, and non-cb5, solely based on Na^+ current amplitude during a step from −70 to −30 mV.

generation threshold equaled 41.9 ± 18.5 pA; the action potential voltage threshold was −46.0 ± 5.8 mV; the voltage at the peak of the action potential equaled −20.5 ± 11.2 mV; Na^+ current amplitude during a step from −70 to −30 mV was −698 ± 325 pA). Three bipolar cells in the sample had Na^+ current transients of −100 to −400 pA and were classified as cb5a type. In one of the cells (Fig. 4*B*), injecting a current larger than 30 pA produced a single, broad (3 ms width at half-height), low amplitude (peak attained voltage = −31.3 mV) spike. For this cell, a plot of peak voltage response versus current injection amplitude (Fig. 4*D*, middle) displayed a nonlinear increase between 30 and 40 pA. The other two putative cb5a cells responded to increasing current injections with an approximately linear change in membrane voltage (Fig. 4*D*, middle). Finally, cells that had negligible initial transients during a voltage-clamp step also responded with a linear increase in membrane voltage during current injections of increasing amplitude (Fig. 4*C*,*D*, bottom, $n = 15$, resting potential = −64.9 ± 5.6 mV, results from 4 representative cells are shown). The current step that elicited a spike in cb5b cells, 35–40 pA, is comparable to the current injected into On bipolar cells during a bright light stimulus at a holding potential of −70 mV (44.7 ± 21.6 pA; $n = 5$ cb5b cells). cb5b action potentials were eliminated by TTX (Fig. 4*E*; $n = 4$), and were thus mediated by Na^+ channels. In contrast, the graded responses of non-cb5 cells commonly had a small TTX-resistant transient (Fig. 4*F*, $n = 6$) that was probably mediated by a voltage-dependent Ca^{2+} current (Protti et al., 2000; Koizumi et al., 2001). In slices, bipolar and ganglion cell action potentials had similar widths, and amplitudes that peaked at between −20 and −10 mV (Fig. 4*G*). Ganglion cell action potentials recorded in retinal flat-mounts routinely exceeded +20 mV, so it is conceivable that cb5b action potentials might also have a larger amplitude in the intact retina. Recordings in these experiments were made in the whole-cell configuration which, when compared with perforated patch recording, provides better temporal resolution, but may also perturb the intracellular milieu and affect cell excitability.

Light flashes produced action potentials in cb5b bipolar cells

We next determined whether dark-adapted cb5b bipolar cells could fire action potentials in response to a light stimulus. On bipolar cell membrane voltage was recorded in the current-clamp configuration. In these experiments, a perforating agent, either amphotericin B or gramicidin D, was included in the pipette solution. Membrane voltage was measured within a few tens of seconds after establishing a gigaseal and remained stable over a 30–60 min experiment during which time pipette resistance typically decreased from 800 to 70 MΩ. We reasoned that the combination of a high pipette resistance and the presence of a perforating agent should retard ion exchange between the pipette solution and the cell cytoplasm, thus preserving the intracellular milieu. The dark resting potential of cb5b cells, identified after experiments by labeling with antibodies against calb and PKC, was −56.0 ± 2.5 mV ($n = 7$, amphotericin as the perforating agent; −53.0 ± 10.0 mV, $n = 3$, gramicidin as the perforating agent), which was significantly more depolarized than the resting potential measured during normal whole-cell recording (Fig. 1*C*; $p < 0.01$).

A more depolarized resting potential during perforated patch recordings should increase the fraction of Na^+ channels in the inactive state, and thus make it more difficult for a depolarizing

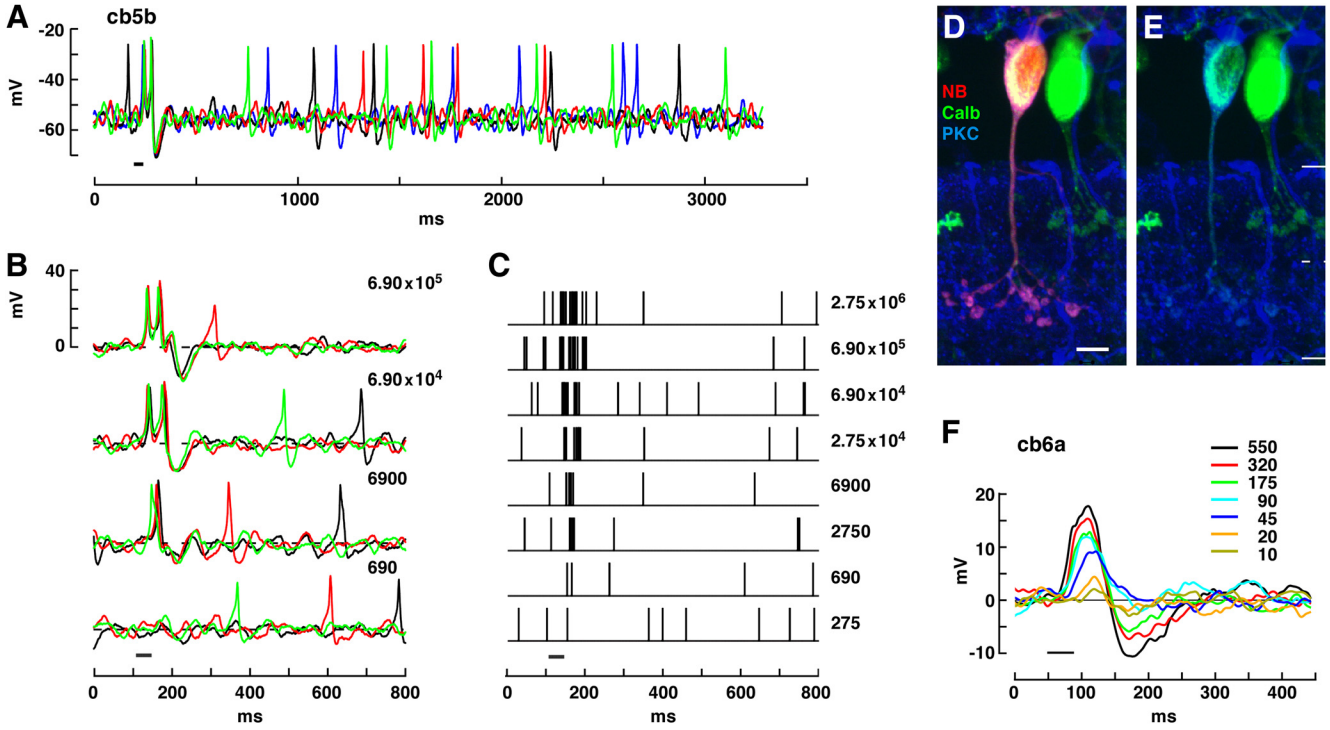

Figure 5. Light flashes elicit all-or-nothing action potentials in a cb5b bipolar cell. ***A***, Spontaneous activity during 4 consecutive traces. A flash (40 ms; horizontal bar) of light delivering 2750 photons-μm^{-2} produced a spike doublet at the start of each trace. The voltage threshold for spike generation was obtained from an inflection point at start of each spike. ***B***, Voltage responses during a series of flashes of increasing intensity (shown at right in units of photons-μm^{-2}). A resting voltage of −55.3 mV was subtracted from the baseline. ***C***, Vertical lines show the time at which a spike occurred. Sum of 9 traces at each intensity. Combined results from two separate repeats of the intensity series occurring between 3.75–20 and 22–42 min after gigaseal formation. Flash intensity in units of photons-μm^{-2}. ***D***, ***E***, At the end of the recording, the cell was filled with Neurobiotin by rupturing the membrane patch that occluded the tip of the whole-cell pipette. The recorded cell was positive for both calb and PKC. At right is a $calb^+$ cb2 bipolar cell. The solid lines show the borders of the IPL, while the dashed line shows the approximate division between sublaminas a and b. ***F***, Voltage response of a cb6a bipolar cell to light flashes of increasing intensity (at the right in units of photons-$\mu m^{-2} \times 10^{-3}$). A flash delivering 46,730 photons-μm^{-2} produced a half-maximal response as determined by fitting a Michaelis-Menten curve to the intensity–response relation. A resting voltage of −48.5 mV was subtracted from the baseline. ***A***--***E*** from one cell. Scale bar, 5 μm.

current pulse to produce a regenerative response. Indeed, we found that pulses of light superimposed on a dark background almost always produced graded membrane depolarizations in cb5b cells. In two exceptional cases, cb5b bipolar cells maintained a low rate of spontaneous firing in the dark, which was increased immediately after a light pulse. Results from one of the cells is shown in Figure 5. This cell maintained a firing rate in the dark of ~3 Hz (Fig. 5*A*). The spikes had a highly reproducible shape, with a threshold to peak amplitude of 30.4 ± 0.4 mV and a width at half-height of 8.8 ± 1.1 ms ($n = 7$ spikes). As the intensity of a 40 ms light flash was increased, the cell generated first a single spike, and then two spikes in succession (Fig. 5*B*). Spike activity following a flash was elevated above background at an intensity of 2750 photons-μm^{-2}, at which time the latency between the start of the stimulus and the first spike was ~60 ms. The average number of spikes per flash was half-maximal at an intensity of ~6900 photons-μm^{-2}, reaching a maximum at $>10^5$ photons-μm^{-2} (Fig. 5*C*). At high intensities, the latency to first spike decreased to 30 ms. A voltage step from −70 to −30 mV elicited a transient current with an amplitude of −275 pA, which is likely to be an underestimate given an uncompensated pipette resistance of 70 MΩ. The recorded bipolar cell was both calb and PKC positive (Fig. 5*D*,*E*), consistent with its identification as a cb5b cell. The spiking responses of the cb5b cell are not characteristic of all On bipolar cell types. For example, an On bipolar cell with a minimal Na^+ current, a cb6a cell, had a large light response (~20 mV; Fig. 5*F*), but did not generate action potential-like transients.

Spike responses of cb5b cells during temporal flicker

Most cb5b cells failed to generate all-or-nothing transients when depolarized from rest by a light stimulus. We noted, however, that the flash responses in some On bipolar cells were biphasic, with an after-hyperpolarization in the range of 10–20 mV below baseline (Fig. 5*A*,*B*,*F*). We reasoned that a brief light stimulus followed by a period of darkness of the appropriate length might produce a hyperpolarization that relieves Na^+ channel inactivation, leading to a spike at rebound during a subsequent stimulus. To test this idea, we applied temporal flicker according to a pseudo-random m-sequence, which contained dark periods of varying lengths, and measured the voltage responses of cb5b and non-cb5b On bipolar cells (Fig. 6). Within 30 s after making a gigaseal, a cb5b cell was observed to rest at −52.2 mV. Subsequently, the slice was illuminated with full field flicker, and the membrane potential began to fluctuate between −50 and −75 mV. During flicker, recovery from hyperpolarization was frequently followed by a 10–20 mV depolarizing transient. These transients were caused by a voltage-dependent Na^+ current since they were attenuated by puffer application of TTX (Fig. 6*A*). This result was obtained early in the recording (~4 min), at a time when a subsequent voltage-clamp measurement demonstrated both poor electrical access (series resistance ~340 MΩ) and the absence of an inward transient corresponding to a Na^+ current (Fig. 6*B*). Pipette series resistance reached a minimum value of 70 MΩ after 20 min of recording. A flickering stimulus produced numerous small (10–20 mV; Fig. 6*C*) and occasional large

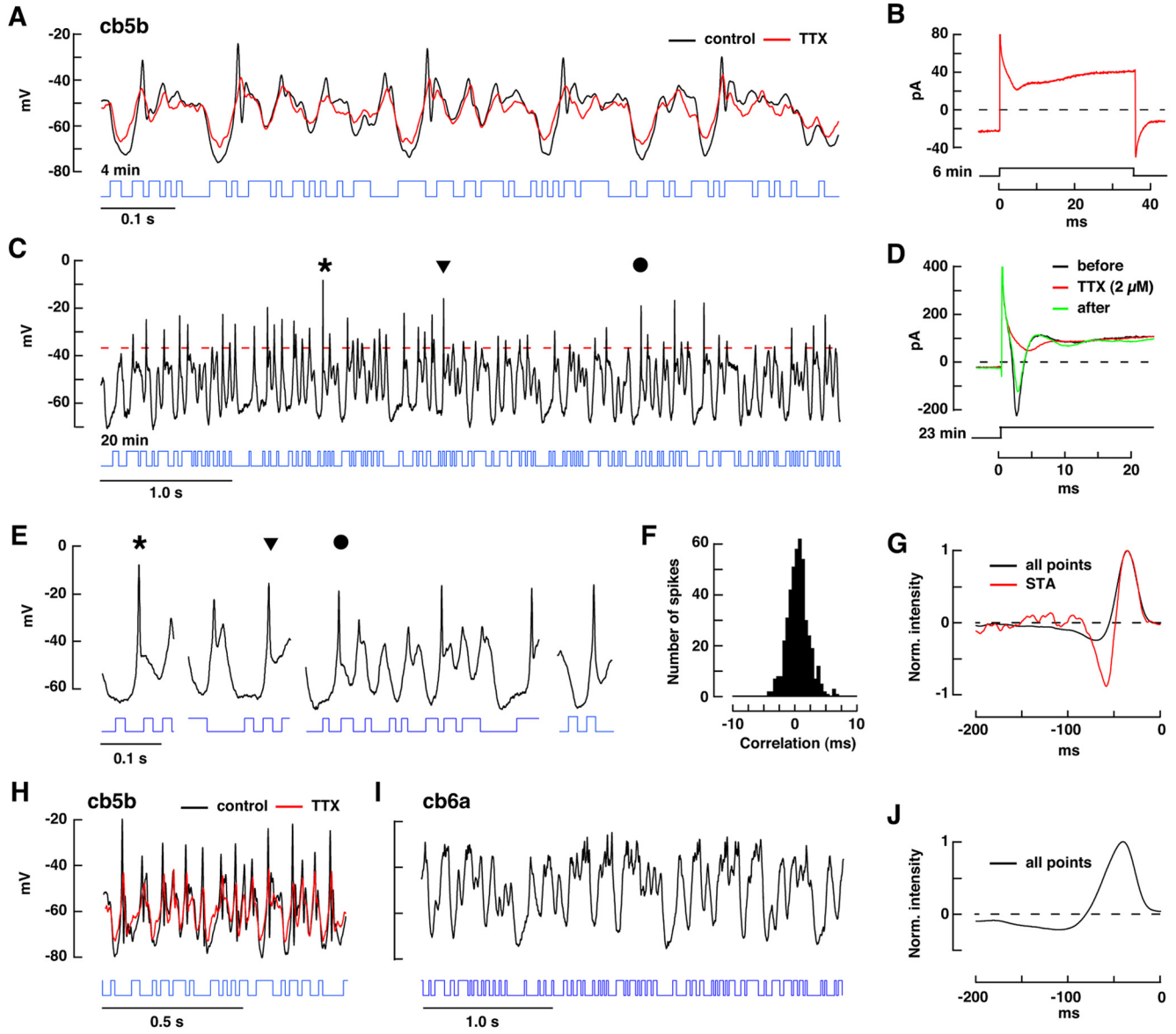

Figure 6. Responses of On bipolar cells to random temporal flicker. ***A***, Voltage response (black trace) of a cb5b cell during random binary flicker (blue trace, below, upward deflection corresponds to light-on; mean intensity equals 3.42×10^6 photons-$\mu m^{-2} s^{-1}$) under control conditions and in the presence of TTX (2 μM, red trace). ***B***, Subsequent current response to a step in voltage clamp from −70 to −30 mV illustrating poor voltage control due to high pipette series resistance (~340 MΩ). ***C***, Extended period of flicker response obtained 20 min after the start of the recording. ***D***, Current response during a step from −70 to −30 mV before, during, and after TTX application. ***E***, Rapid depolarizing transients from ***C*** presented on a faster time base. Symbols show corresponding regions. The fourth sample was obtained at a later time during this continuous 15 s run. ***F***, Spike timing during three consecutive traces stimulated with identical flicker sequences. ***G***, Linear filters obtained using all of the response points (black trace) or just the points corresponding to the occurrence of spikes (STA, red trace). ***H***, Flicker response from a different cb5b cell which showed discrete spikes that were suppressed by TTX. Gramicidin perforated patch recording. ***I***, Purely graded flicker responses in a cb6a bipolar cell. ***J***, Linear filter for the cb6a cell. Time in minutes (***A–D***) corresponds to the time after the start of data acquisition, which commenced soon after formation of the gigaseal.

(30–40 mV; Fig. 6*C*,*E*) spikes. With the spike threshold set to −36.6 mV (Fig. 6*C*; red dashed line; 12 mV above the dark resting potential), the spike rate during the 15 s stimulus averaged 8.6 Hz. After obtaining flicker data, the amplitude of the Na^+ current was measured by stepping the membrane potential from −70 to −30 mV in both the absence and presence of TTX. The current obtained by subtraction had a peak amplitude of −315 pA (Fig. 6*D*). This is likely an under estimate due to an uncompensated pipette resistance. The largest spikes in the train (Fig. 6*E*) had an amplitude measured from threshold inflection to peak of 30.8 ± 3.9 mV, attained a peak voltage of −16.6 ± 3.7 mV, and had a width at half-height of 3.0 ± 0.3 ms ($n = 8$ spikes). The temporal reliability of the spikes was measured by repeating the same m-sequence stimulus. Spike rate varied by <15% between stimulus repeats, and spike timing was tightly regulated to within 2.23 ± 0.27 ms (Gaussian fit to the histogram in Fig. 6*F*; Gaussian mean ± SD = −0.2 ± 0.6 ms; $n = 6$).

We used the m-sequence stimulus and either the bipolar cell voltage trace or a spike-binarized version of the trace to calculate a linear filter for the light response (Fig. 6*G*). The linear filter provides information about the average light stimulus that precedes either a membrane depolarization or spike, respectively. If the spikes and graded signals respond to the same stimuli, the filters should have a similar shape. However the filter obtained from spikes was dramatically more biphasic that the "all-points" filter (biphasic index of 1.0 ± 0.17 vs 0.32 ± 0.9; $n = 4$ cells) and

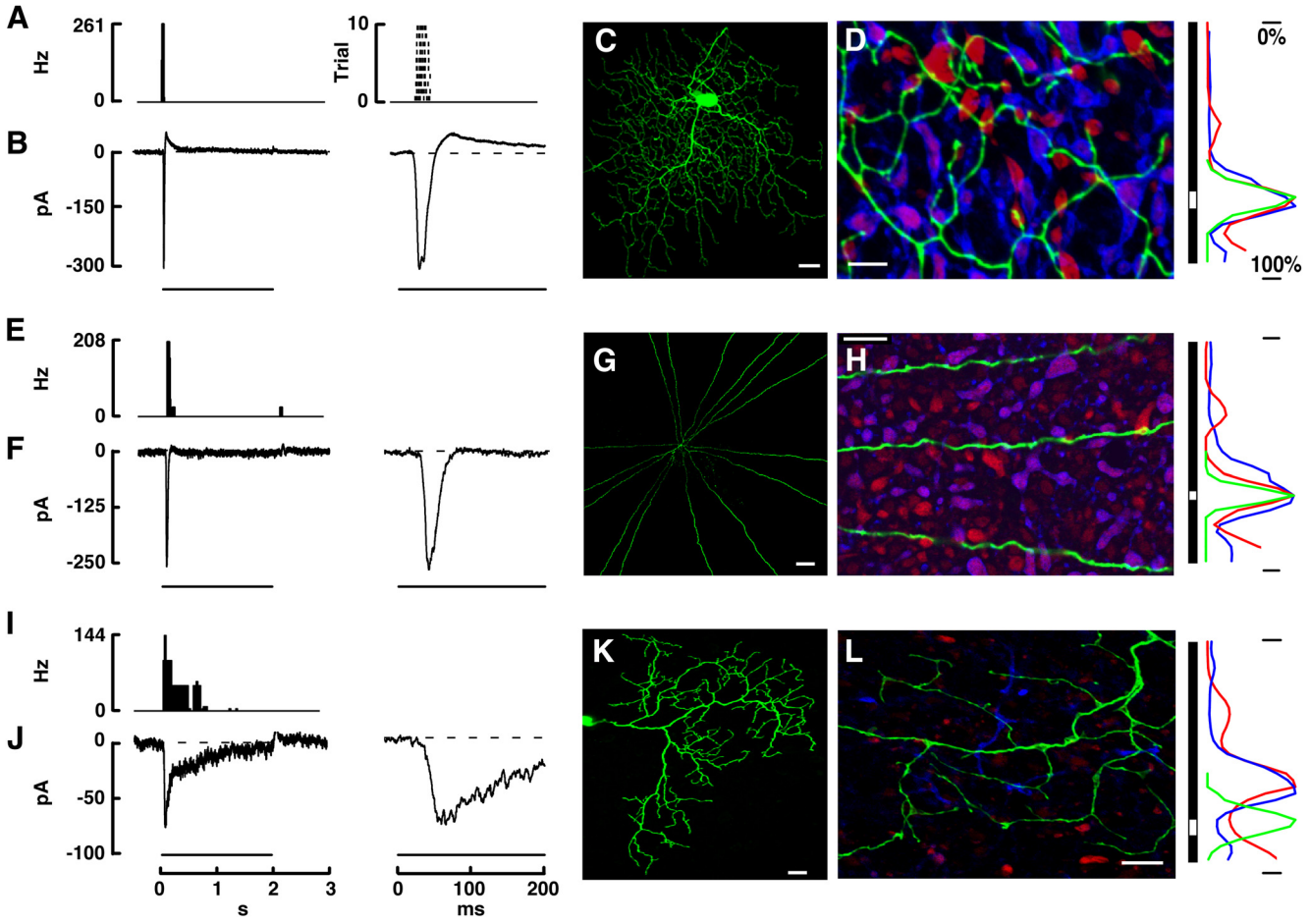

Figure 7. The axon terminals of cb5a/b cells costratify with the dendrites of On transient amacrine and ganglion cells. ***A***, Left, Peristimulus histogram showing the spike rate in Hz of a single ganglion cell during a 2 s flash of light (lower horizontal bar in ***B***, left). Bin width = 20 ms. Right, Raster plot showing the time of spike occurrence during 10 consecutive stimulus presentations on a faster time base. ***B***, Left, Light-evoked EPSC recorded in the whole-cell configuration at a membrane potential of −70 mV. (right). EPSC response on a faster time base. ***C***, Confocal image of a flat-mounted retina showing the tracer-labeled ganglion cell. ***D***, Left, A 2-μm-thick optical section at the level of the dendrites of the Neurobiotin-labeled ganglion cell (green). cb5b cell terminals were labeled by antibodies to PKC (blue) and calb (red), whereas cb5a cell terminals were labeled only by calb. Right, Intensity of Neurobiotin (green), PKC (blue), and calb (red) labeling plotted as a function of IPL depth from top, 0%, to bottom, 100%. The white bar indicates the level of the image in ***D***. ***E***, Peristimulus spike histogram from another cell. ***F***, Light-evoked EPSC on a slow (left) and fast (right) time base. ***G***, The wide-field amacrine cell had neurites (***H***) that narrowly ramified within the layer formed by cb5a/b cell terminals. ***I***, ***J***, Peristimulus histogram and EPSC light responses for a ganglion cell with a relatively sustained response. ***K***, ***L***, Ganglion cell dendrites ramified between the band formed by cb5a/b cell terminals and the bottom of the IPL.

had a more rapid time course as judged by the time to zero-crossing (−39.7 ± 6.1 vs −46.0 ± 6.1 ms). Both inspection of the raw voltage traces and the spike-triggered average filter suggests that spikes preferentially occurred after a transition to light that is preceded by a period of dark. Similar results were obtained in a total of 4 bipolar cells that either had large Na^+ currents or were calb and PKC positive, or both. A flicker response from a another cell in the sample is shown in Figure 6*H*, illustrating both large spikes in control conditions and near complete block of spikes by TTX. As a control, we recorded the flicker responses of 3 On bipolar cells that lacked Na^+ currents. The responses of one of the cells, a cb6a, is shown in Figure 6*I* (same cell as in Fig. 5*F*). The flicker responses showed a dynamic range of >30 mV, but did not demonstrate rebound spikes. The linear filter was slower and more monophasic than that of the cb5b cell (zero crossing at −115 ms and biphasic index = 0.23).

Cb5 cell terminals costratify with transient-responding On ganglion cell dendrites

On transient ganglion cells fire a burst of spikes with a short latency at the start of a light pulse. Cb5b cells also spiked with a short latency (~30 ms) at the start of a bright light pulse (Fig. 5*B*). Thus, we next wanted to test whether the axon terminals of cb5b cells costratified in the IPL with the dendrites of On transient amacrine and ganglion cells. Costratification does not imply synaptic communication, but it is a prerequisite for rapid and robust signaling. To record ganglion cell light responses, we switched to a retinal flat-mount preparation. The effect of light on the spike responses of ganglion cells was first measured in the on-cell configuration. The ganglion cell whose responses are shown in Figure 7*A* fired a high-frequency burst of spikes at light onset. The cell membrane occluding the pipette tip was subsequently ruptured allowing the contents of the pipette solution to diffuse into the cell. The pipette solution contained pharmacological agents that minimized voltage-dependent membrane currents. Membrane voltage was maintained at −70 mV, the Cl^- reversal potential of the pipette solution, to isolate the EPSCs that result from bipolar cell glutamate release. A bright light stimulus produced an EPSC with a peak amplitude of −300 pA, a width at half-height of 15.0 ms, and a latency to first spike of 24.4 ms (Fig. 7*B*). After the experiment, the tissue was fixed and labeled for Neurobiotin, calb, and PKC (Fig. 7*C*,*D*). A 2-μm-thick *z*-stack delimited by the

labeled terminals of cb5b and cb5a cells also encompassed the dendrites of the labeled ganglion cell. A plot of label intensity versus IPL depth demonstrated near complete costratification (Fig. 7*D*, right). A second cell type, a wide field amacrine (WFA) cell, also had a transient EPSC and dendrites that costratified with the terminals of cb5a/b bipolar cells. The WFA cell whose responses are shown in Figure 7*E–H* produced a narrow burst of spikes at light onset and had a correspondingly narrow EPSC width (31.2 ms at half-height; latency to first spike = 36.0 ms). WFA cells had long uniform processes that initially branched at or near the soma, and which likely function in both signal input and output. These neurites ramified in a very narrow band in the center of the layer comprised of cb5a/b cell terminals (Fig. 7*H*; 100% overlap). Altogether, we recorded from 6 ganglion and amacrine cells with transient responses (31.1 ± 18.0 ms peak width at half-height; 38.7 ± 16.5 ms latency to first spike) and near complete (99.5%) overlap with cb5a/b cell axon terminals. For comparison, we also recorded from 4 ganglion cells with dendrites that had significantly less overlap with the axon terminals of cb5a/b bipolar cells (Fig. 7*I–L*; 35 ± 21% overlap, significantly different from the transient group, $p < 0.01$). These cells fired spikes during a broad interval at the start of the light stimulus and had EPSCs that were significantly wider than those of transient responding cells (435.8 ± 426 ms peak width at half-height, $p < 0.01$; excluding an usually sustained response of width 1040 ms, the mean width of the sample, 234.4 ± 171 ms, still differed significantly from that of the transient group, $p < 0.02$; 45.7 ± 15.3 ms latency to first spike, not significantly different from the transient group). The results are consistent with the idea that a spiking bipolar cell provides input to amacrine and ganglion cells that signal with transient responses.

Discussion

Subsets of bipolar cells in amphibian, teleost, and mammalian retinas contain transient Na^+ currents. However, it has been unclear whether these currents functioned only to augment graded light responses (Pan and Hu, 2000; Ichinose et al., 2005) or could generate all-or-nothing action potentials (Ma et al., 2005; Ichinose and Lukasiewicz, 2007; Cui and Pan, 2008). We show that cb5b bipolar cells are unique among ground squirrel bipolar cells in that Na^+ currents are, on average, −600 pA, but can exceed −1000 pA during a −70 to −30 mV step. In response to a light stimulus, the Na^+ currents in cb5b bipolar cells mediate action potentials of up to 40 mV in amplitude. In obtaining these results, we anticipated two problems: First, that whole-cell recording might modify cell excitability; and second, that slicing would perturb bipolar cell function.

To address the concern that whole-cell recording might modify cell excitability, we used perforated patch recording to measure bipolar cell spikes during light stimulation. Perforated patch recording should slow or prevent ion exchange between the pipette and the intracellular milieu, especially early in the experiment when pipette series resistance is high. With amphotericin B as the perforating agent, a resting membrane voltage of −56.0 ± 2.5 mV was obtained within 30 s of forming a gigaseal when pipette series resistance was >800 MΩ. This hyperpolarized resting voltage was stable during a 30–60 min recording (Fig. 6*A*, *C*) during which time series resistance declined to ~70 MΩ. The integrity of the perforated patch was assessed by monitoring the pipette series resistance during a recording. Accidental rupture, signified by an abrupt drop in series resistance, was followed by a quick membrane hyperpolarization down to the same resting level obtained during standard whole-cell recordings, −67 mV. From the stability throughout the recording period, we infer that the relatively positive resting potential measured during the perforated patch recordings more closely approximates the *in vivo* condition. A more positive resting potential increases Na^+ current inactivation and should reduce the likelihood that a flash of light will cause an action potential. Indeed, flashes of light on a dark background resulted in cb5b action potentials in only two recordings. Surprisingly, a flickering light stimulus resulted in a steady rate of action potential generation. The flickering stimulus produced membrane hyperpolarizations to −65 or −70 mV which lasted for 30–50 ms. Evidently, enough Na^+ channel inactivation was removed during these negative excursions so that a subsequent depolarization by light could produce an action potential.

To address the issue of damage due to slicing, we measured the sensitivity of 15 On and 2 Off ground squirrel bipolar cells during perforated patch recordings. The intensity that produced a half-maximal light response ranged from 460 to 144,600 photons-μm^{-2} for a 40 ms flash, with a median value of 3360 and a mean of 5530 ± 4820 (excluding the three highest and lowest values). The measured bipolar cell sensitivity compares favorably with that in the green cones of the golden mantled ground squirrel ($I_{1/2}$ = 10,900 photons-μm^{-2}; Kraft, 1988), which attests to the integrity of the cone to bipolar cell synapses in our slices. Nonetheless, we cannot exclude that slicing reduces presynaptic inhibition at the bipolar cell terminal by severing the neurites of wide-field amacrine cells. The consequences of reducing presynaptic inhibition are hard to predict. A reduction in tonic inhibition might enhance membrane excitability and thus action potential generation during a light stimulus. Alternatively, the reduction may produce an additional membrane depolarization that leads to increased Na^+ channel inactivation, making it more difficult to generate action potentials.

A further test that action potentials occur during light involves recording from the ganglion cells that receive excitatory input from cb5b cells in the flat-mounted retina. We tried to isolate a TTX-sensitive component of excitatory input into ganglion cells, but our results were inconclusive. There were at least three impediments to obtaining a positive result. First, we had no strategy for targeting On transient ganglion and WFA cells, and thus recordings from these cell types were relatively rare. Second, recordings were done in a solution that contained picrotoxin and strychnine to block the TTX-sensitive amacrine cell inputs to bipolar cell terminals (Demb et al., 2001); however, both agents may depolarize bipolar cells, reducing the likelihood of their firing an action potential. And third, the isolation of a TTX-sensitive component in the excitatory input to a ganglion cell does not immediately indicate that the component arises from a spiking rather than a graded response. Voltage-clamp recordings from flat-mounted guinea pig and mouse retina suggest that a TTX-sensitive Na^+ current plays a minor role in shaping the excitatory bipolar cell input to On transient ganglion cells (Demb et al., 1999; Demb et al., 2001; Tian et al., 2010). We can only speculate that the experiments on mice and guinea pigs either did not use the appropriate stimuli for eliciting action potentials or that the bipolar cells in these species do not generate action potentials. In mice, low mesopic stimuli may not have provided optimal drive to the cone bipolar cells that contain Na^+ channels (Tian et al., 2010). In addition, the Na^+ currents in rodent type 5 bipolar cells are smaller than those in ground squirrel cb5b cells (<150 pA), and did not generate spikes in response to a light flash (Cui and Pan, 2008). In the guinea pig, the temporal characteristics of the square wave stimulus might not have been optimal to

elicit bipolar cell action potentials, although light levels and stimulus contrast were probably adequate (Demb et al., 1999, 2001).

What is the function of bipolar cell Na^+ spikes? Na^+ spikes most frequently occurred during temporal flicker. Raw voltage responses (Fig. 6*A*,*C*,*E*,*H*) show that spikes tended to follow a period of darkness that lasted >30 ms followed by a period of light. The spike-triggered average response showed both that a marked transition from dark to light consistently preceded a spike and that the stimulus that preceded a spike was, on average, different from the stimulus that preceded a graded depolarization (Fig. 6*G*). The implication is that spikes and graded responses encode different visual stimuli. On the idea that cb5b cell action potentials signal swift and marked transitions from dark to light, we characterized the responses of amacrine and ganglion cells whose dendrites costratified with cb5 cell terminals. We found that the same lamina contained the terminals of cb5 cells and the dendrites of ganglion and WFA cells that signaled dark to light transitions with a rapid burst of spikes. On ganglion cells that terminated elsewhere had more prolonged responses. Teleost bipolar cells can generate all-or-nothing Ca^{2+} transients in response to light (Protti et al., 2000; Dreosti et al., 2011), but these events are slower than the Na^+ transients we describe, and are unlikely to function in a pathway that signals rapid change.

The faithful transmission of a spike-like depolarization to amacrine and ganglion cells will depend upon the time- and voltage-dependent properties of synaptic Ca^{2+} currents. Release from both goldfish Mb1 and rat rod bipolar cell terminals is mediated by a rapidly activating L-type Ca^{2+} current (Mennerick and Matthews, 1996, 1998; Singer and Diamond, 2003), although T-type currents may play a role outside of the physiological voltage range (Pan et al., 2001; Singer and Diamond, 2003). Ca^{2+} channel gating and release are fast enough to occur during a 1–2 ms duration action potential. A similarly rapid release is expected in cone bipolar cells, although whether L- or T-type channels separately or together gate release is not clear from studies in primary culture (Hu et al., 2009). In ground squirrel slices, On cone bipolar cells ($n = 18$, including 3 cb5 cells) generated a large (-151 ± 48 pA), sustained, dihydropyridine-sensitive (50 μM isradipine, $n = 8$; Hof et al., 1984) current with L-type properties (Light, 2009). The L-type current attained half-maximal activation at -51.1 ± 2.2 mV ($n = 18$; Light, 2009), a value that is well suited to mediate transmitter release from cb5b cells during both graded and transient events. Given a common postsynaptic target, we assume that the release from both graded and transient events sum.

Graded neurons can encode and transmit information at steady rates that exceed those in action potential generating neurons (de Ruyter van Steveninck and Laughlin, 1996; Juusola and French, 1997). A greater information capacity may enable cells of the outer retina to more efficiently compare and process spatial patterns of illumination, for example, over the receptive field center and surround. Even in the ground squirrel, graded processing predominates in bipolar cells. However, graded processing may constrain the speed at which signals propagate through retinal circuits. cb5b cell action potentials come at the start of a flash response and may promote an earlier, more vigorous response in ganglion cells. Such responses could be useful for signaling sudden movement within the visual field.

References

Akaike N (1996) Gramicidin perforated patch recording and intracellular chloride activity in excitable cells. Prog Biophys Mol Biol 65:251–264.

Barlow HB (1953) Summation and inhibition in the frog's retina. J Physiol 119:69–88.

Baylor DA, Fettiplace R (1977) Kinetics of synaptic transfer from receptors to ganglion cells in turtle retina. J Physiol 271:425–448.

Baylor DA, Fuortes MG (1970) Electrical responses of single cones in the retina of the turtle. J Physiol 207:77–92.

Cuenca N, Deng P, Linberg KA, Lewis GP, Fisher SK, Kolb H (2002) The neurons of the ground squirrel retina as revealed by immunostains for calcium binding proteins and neurotransmitters. J Neurocytol 31:649–666.

Cui J, Pan ZH (2008) Two types of cone bipolar cells express voltage-gated Na+ channels in the rat retina. Vis Neurosci 25:635–645.

Dawis SM (1981) Polynomial expressions of pigment nomograms. Vision Res 21:1427–1430.

de Ruyter van Steveninck RR, Laughlin SB (1996) Light adaptation and reliability in blowfly photoreceptors. Int J Neural Syst 7:437–444.

Demb JB, Haarsma L, Freed MA, Sterling P (1999) Functional circuitry of the retinal ganglion cell's nonlinear receptive field. J Neurosci 19:9756–9767.

Demb JB, Zaghloul K, Haarsma L, Sterling P (2001) Bipolar cells contribute to nonlinear spatial summation in the brisk-transient (Y) ganglion cell in mammalian retina. J Neurosci 21:7447–7454.

DeVries SH (2000) Bipolar cells use kainate and AMPA receptors to filter visual information into separate channels. Neuron 28:847–856.

DeVries SH, Li W, Saszik S (2006) Parallel processing in two transmitter microenvironments at the cone photoreceptor synapse. Neuron 50:735–748.

Dowling JE, Ripps H (1973) Effect of magnesium on horizontal cell activity in the skate retina. Nature 242:101–103.

Dreosti E, Esposti F, Baden T, Lagnado L (2011) In vivo evidence that retinal bipolar cells generate spikes modulated by light. Nat Neurosci 14:951–952.

Helgen KM, Cole FR, Helgen LE, Wilson DE (2009) Generic revision in the holarctic ground squirrel genus *Spermophilus*. J Mammalogy 90:270–305.

Hille B (2001) Ion channels of excitable membranes, Ed 3. Sunderland, MA: Sinauer Associates, Inc.

Hof RP, Scholtysik G, Loutzenhiser R, Vuorela HJ, Neumann P (1984) PN 200–110, a new calcium antagonist: electrophysiological, inotropic, and chronotropic effects on guinea pig myocardial tissue and effects on contraction and calcium uptake of rabbit aorta. J Cardiovasc Pharmacol 6:399–406.

Hu C, Bi A, Pan ZH (2009) Differential expression of three T-type calcium channels in retinal bipolar cells in rats. Vis Neurosci 26:177–187.

Ichinose T, Lukasiewicz PD (2007) Ambient light regulates sodium channel activity to dynamically control retinal signaling. J Neurosci 27:4756–4764.

Ichinose T, Shields CR, Lukasiewicz PD (2005) Sodium channels in transient retinal bipolar cells enhance visual responses in ganglion cells. J Neurosci 25:1856–1865.

Juusola M, French AS (1997) The efficiency of sensory information coding by mechanoreceptor neurons. Neuron 18:959–968.

Kaneko A (1970) Physiological and morphological identification of horizontal, bipolar and amacrine cells in goldfish retina. J Physiol 207:623–633.

Koizumi A, Watanabe SI, Kaneko A (2001) Persistent Na+ current and Ca^{2+} current boost graded depolarization of rat retinal amacrine cells in culture. J Neurophysiol 86:1006–1016.

Kraft TW (1988) Photocurrents of cone photoreceptors of the golden-mantled ground squirrel. J Physiol 404:199–213.

Lasater EM (1986) Ionic currents of cultured horizontal cells isolated from white perch retina. J Neurophysiol 55:499–513.

Li W, DeVries SH (2006) Bipolar cell pathways for color and luminance vision in a dichromatic mammalian retina. Nat Neurosci 9:669–675.

Light AC (2009) Transient and sustained off bipolar cells in the ground squirrel retina. PhD thesis, Northwestern University.

Linberg KA, Suemune S, Fisher SK (1996) Retinal neurons of the California ground squirrel, *Spermophilus beecheyi*: a Golgi study. J Comp Neurol 365:173–216.

Ma YP, Cui J, Pan ZH (2005) Heterogeneous expression of voltage-dependent Na^+ and K^+ channels in mammalian retinal bipolar cells. Vis Neurosci 22:119–133.

Mennerick S, Matthews G (1996) Ultrafast exocytosis elicited by calcium current in synaptic terminals of retinal bipolar neurons. Neuron 17:1241–1249.

Mennerick S, Matthews G (1998) Rapid calcium-current kinetics in synaptic terminals of goldfish retinal bipolar neurons. Vis Neurosci 15:1051–1056.
Pan ZH, Hu HJ (2000) Voltage-dependent Na(+) currents in mammalian retinal cone bipolar cells. J Neurophysiol 84:2564–2571.
Pan ZH, Hu HJ, Perring P, Andrade R (2001) T-type Ca(2+) channels mediate neurotransmitter release in retinal bipolar cells. Neuron 32:89–98.
Protti DA, Flores-Herr N, von Gersdorff H (2000) Light evokes Ca^{2+} spikes in the axon terminal of a retinal bipolar cell. Neuron 25:215–227.
Puller C, Ondreka K, Haverkamp S (2011) Bipolar cells of the ground squirrel retina. J Comp Neurol 519:759–774.
Reid RC, Victor JD, Shapley RM (1997) The use of m-sequences in the analysis of visual neurons: linear receptive field properties. Vis Neurosci 14:1015–1027.
Schroeder MR (2009) Number theory in science and communication: with applications in cryptography, physics, digital information, computing, and self-similarity, 5th Ed. Berlin: Springer.
Shingai R, Christensen BN (1983) Sodium and calcium currents measured in isolated catfish horizontal cells under voltage clamp. Neuroscience 10:893–897.
Shingai R, Christensen BN (1986) Excitable properties and voltage-sensitive ion conductances of horizontal cells isolated from catfish (*Ictalurus punctatus*) retina. J Neurophysiol 56:32–49.
Singer JH, Diamond JS (2003) Sustained Ca^{2+} entry elicits transient postsynaptic currents at a retinal ribbon synapse. J Neurosci 23:10923–10933.
Szmajda BA, DeVries SH (2011) Glutamate spillover between mammalian cone photoreceptors. J Neurosci 31:13431–13441.
Tian M, Jarsky T, Murphy GJ, Rieke F, Singer JH (2010) Voltage-gated Na channels in AII amacrine cells accelerate scotopic light responses mediated by the rod bipolar cell pathway. J Neurosci 30:4650–4659.
Werblin FS, Dowling JE (1969) Organization of the retina of the mudpuppy, *Necturus maculosus*. II. Intracellular recording. J Neurophysiol 32:339–355.
West RW (1976) Light and electron microscopy of the ground squirrel retina: functional considerations. J Comp Neurol 168:355–377.
Zenisek D, Henry D, Studholme K, Yazulla S, Matthews G (2001) Voltage-dependent sodium channels are expressed in nonspiking retinal bipolar neurons. J Neurosci 21:4543–4550.